Pharmaceutical Research, Vol. 24, No. 4, April 2007 (© 2007)
DOI: 10.1007/s11095-006-9190-3

Research Paper

Antiangiogenic and Apoptotic Properties of a Novel Amphiphilic Folate-Heparin-Lithocholate Derivative Having Cellular Internality for Cancer Therapy

Mi Kyung Yu,[1,★] Dong Yun Lee,[2,★] Yoo Shin Kim,[3] Kyeongsoon Park,[4] Soo Ah Park,[5] Dai Hyun Son,[5] Gee Young Lee,[6] Jong Hee Nam,[7] Sang Yoon Kim,[5] In San Kim,[3] Rang Woon Park,[3] and Youngro Byun[2,8]

Received October 16, 2006; accepted November 7, 2006; published online February 21, 2007

Purpose. Anitangiogenic and apoptotic properties of a novel chemically modified heparin derivative with low anticoagulant activity were evaluated on the experimental *in vitro* and *in vivo* model.
Materials and Methods. Heparin-lithocholate conjugate (HL) was initially synthesized by covalently bonding lithocholate to heparin. Folate-HL conjugate (FHL) was further synthesized by conjugating folate to HL. Antiangiogenic and apoptotic abilities of HL and FHL were characterized in vitro and *in vivo* experimentations.
Results. Compared to unmodified heparin, both HL and FHL represented a low anticoagulant activity (38 and 28%, respectively). HL and FHL maintained antiangiogenic activity even further modification from the results of Matrigel plugs assay. FHL specifically induced apoptosis on KB cells having highly expressed folate receptor after cellular internalization. Both administered HL and FHL had similar antiangiogenic activity and inhibitory effect on tumor growth *in vivo* although FHL induced higher apoptosis on tumor tissues.
Conclusions. *In vivo* tumor growth inhibition was possibly due to the decrease of vessel density and apoptotic cell death, although antiangiogenic effect of FHL seemed more actively affected on growth inhibition than apoptotic potential *in vivo* system. Thus, Low anticoagulant FHL having antiangiogenic and apoptotic properties would provide benefits for the development of a new class of anticancer agent.

KEY WORDS: antiangiogenesis; apoptosis; folate-heparin-lithocholate; tumor growth.

INTRODUCTION

Recent evidences are accumulated that heparin, a highly sulfated polysaccharide belonging to the family of glycosaminoglycan, has anti-tumor activities (1–3). In fact, the treatment with heparin in cancer patients was formerly performed to treat venous thrombosis, and this has led to the observations in large volume of clinical trials that the medical effect of heparin also prolongs cancer patient's survival (4). Diverse effects of heparin on malignant process are mostly based on its inhibition of angiogenic factors, such as bFGF, or interference of metastatic process containing heparanase or selectin mediated cell invasion, and to a lesser extent, on the activity to impede tumor growth and possibly carcinogenesis itself. In addition, several other observations for the apoptotic activities of heparin have been reported (5,6). For example, heparin inhibits activator protein-1, which is the nuclear target of many oncogenic signal transduction pathways (7), and it may bind with DNA through charge to charge interaction; in turn, transcription factors can be upregulated in both the cytosol and the nucleus (8).

Despite these known benefits of heparin for cancer treatment, the strong anticoagulant activity of heparin is a limitation for the clinical applications of heparin at high dose and for long-term treatment in cancer therapy (9). Furthermore, it is still hard to determine the ultimate effect of heparin on cancer progression due to the wide variety of its physiological activities (2,4,10). Although several effective approaches for using sulfated oligosaccharides (11) or chemically modified heparins, such as polystyrene bearing and steroid conjugated heparin (12,13), terminally alkylated heparin (14), have been investigated as angiogenesis inhib-

★ These authors contributed equally to this work as first authors.
[1] Department of Life Science, Gwangju Institute of Science and Technology, Gwangju 500-712, South Korea.
[2] College of Pharmacy, Seoul National University, San 56-1, Sillim-dong, Gwanak-gu, Seoul 151-742, South Korea.
[3] Department of Biochemistry, School of Medicine, Kyungpook National University, Daegu 700-422, South Korea.
[4] Biomedical Research Center, Korea Institute of Science and Technology, Seoul 136-791, South Korea.
[5] Department of Otolaryngology, Asan Medical Center, College of Medicine, University of Ulsan, Seoul 138-736, South Korea.
[6] Department of Materials Science and Engineering, Gwangju Institute of Science and Technology, Gwangju 500-712, South Korea.
[7] Department of Pathology, School of Medicine, Chonnam National University, Gwangju 500-757, South Korea.
[8] To whom correspondence should be addressed. (e-mail: yrbyun@snu.ac.kr)

ABBREVIATIONS: bFGF, basic fibroblast growth factor; FBS, fetal bovine serum; FHL, folate-heparin-lithocholate; FITC, fluorescein isothiocyanate; FR, folate receptor; HL, heparin-lithocholate; MTT, (3-[4,5-dimethylthiazol-2-yl]-2,5-diphenyltetrazolium bromide); PBS, phosphate buffered saline; PI, propidium iodide; TUNEL, terminal deoxynucleotidyl transferase-mediated dUTP nick end-labeling; UFH, unfractionated heparin.

itors or anti-tumor agents, most of technologies were addressed on only angiogenesis, and they required high doses causing the negative effects discussed above.

The folate receptor (FR) is a high-affinity, membrane-anchored protein which mediates the transport of folic acid and its conjugates into the cell interior by endocytosis. Excessive need of rapidly dividing malignant cells for folates may be a reason for the frequent overexpression of FRs in various cancer types such as ovarian, endometrial, breast, nasopharyngeal, renal and colorectal cancers (15–19).Therefore, folate has been identified as the prototype of a "Trojan horse" approach to specific tumor targeting for diagnostic and therapeutic purpose (20,21). Here, we identified the ability of novel heparin derivatives that have antiangiogenic activities combined with apoptotic characteristics for the enhanced tumor target system. In this study, we developed to see if the internalization of heparin could induce apoptosis in cancer cells, and developed low anticoagulant heparin amphiphiles, namely, heparin-lithocholic acids conjugate (HL) and folate conjugated HL (FHL). The antiangiogenesis and apoptosis effects of HL and FHL were evaluated *in vitro* and *in vivo* experimentations.

MATERIALS AND METHODS

Chemicals

Unfractionated heparin (UFH, 167 IU/mg), whose average molecular weight was about 12 kDa, was purchased from Pharmacia Heparin Co. (Franklin, OH). Lithocholic acid, folic acid, ethylenediamine, anhydrous dimethylformamide (DMF), 1-ethyl-3-(3-dimethylaminopropyl) carbodiimide (EDAC) and anhydrous formamide were purchased from Sigma Chemical Co. (St. Louis, MO). *N*-hydroxysuccinimide (NHS), *N*,*N*-dicyclohexyl carbodiimide (DCC), dimethyl sulfoxide (DMSO) and *N*,*N*-diisopropylethylamine (DIEA) were purchased from Aldrich Chemical Co. (Milwaukee, WI). Acetone and methanol were obtained from Merck (Darmstadt, Germany). Acetonitrile was purchased from Junsei Chemical Co. (Tokyo, Japan) and all reagents were of analytical grade and were used without further purification.

Synthesis and Characterization of HL and FHL

Heparin-lithocholate (HL) was synthesized by coupling heparin with the bile analogue, *N*-lithocholylethylamine (Litho-NH_2), as described previously (22). In brief, heparin (100 mg) was dissolved in 3 ml of formamide by gentle heating. EDAC (96 mg) was mixed with the heparin solution, followed by mixing with Litho-NH_2 in DMF (10 ml). This reaction was carried out at room temperature under a nitrogen atmosphere for 24 h. After the mixture was precipitated in excess cold acetone, the precipitate was washed with cold acetone to remove the unreacted Litho-NH_2, and dried in vacuum. Dried HL was suspended in water and lyophilized to produce as white powder. The presence of lithocholic acid in HL and amide linkage were confirmed by ^{1}H NMR (400 MHz, CD_3OD/D_2O=2/1, v/v, JEOL, Tokyo, Japan).

Folate-heparin-lithocholate (FHL) was prepared as follows; folic acid (1 mmol) dissolved in 20 ml DMSO was reacted with DCC (1.2 mmol) and NHS (2 mmol) at 50°C for 6 h. It is generally known that folate has two α- (high affinity for the FR) and γ-carboxylic acids, but the γ-carboxylic acid is more selectively activated due to its higher reactivity (23,24). The resulting folate-NHS was reacted with ethylenediamine (13 mmol) and pyridine (500 mg) at room temperature overnight. The folylethylamine (folate-NH_2) was precipitated by the addition of excess acetonitrile, and the precipitate was filtered and washed with diethyl ether before drying under vacuum to get yellow powder. This was added to the prepared HL (100 mg), dissolved in 20 ml of formamide, and activated by EDAC (3.38 mg) with 5 μl of DIEA for 12 h. The unreacted folate-NH_2 was removed by dialysis (MWCO 2000). The final product, FHL, was obtained by freeze-drying at a yield of 97%. The folate content in FHL was determined by quantitative UV spectrophotometry at 365 nm. The anticoagulant activities of HL and FHL were measured by FXa chromogenic assay (COATEST®Heparin, Milano, Italy) (25).

In Vivo Matrigel Plug Assay

In vivo Matrigel plug assay was performed as previously described (26). Briefly, Matrigel solution (0.67 ml) containing bFGF (500 ng/ml) with 100 μg/ml of heparin derivatives (UFH, HL or FHL, respectively,) was injected subcutaneously into the flank of male C57BL/6 mice (Samtako Bio Korea; Osan, Korea). The injected Matrigel rapidly formed a single gel plug. After 10 days, mice were sacrificed and the Matrigel plugs were removed, fixed with 4% paraformaldehyde, and embedded in paraffin. The plugs were sectioned and examined with H&E staining for microscopic observation.

To quantify the formation of new blood vessels, the amount of hemoglobin (Hb) was measured using Drabkin reagent kit (Sigma). The concentration of Hb was calculated from a known amount of Hb provided by the kit in parallel according to the supplier's protocol. The experiment was repeated four times independently. Investigations using experimental animals adhered to the "Principles of Laboratory Animal Care" (NIH publication #85-23, revised in 1985).

Cell Viability

KB cells (human, nasopharyngeal carcinoma cell line) known to have amplified FR-α expressions were cultured in RPMI 1640 medium (Gibco, Grand Island, NY) containing 10% FBS and 1% penicillin streptomycin at 37°C in a humidified atmosphere of 5% CO_2 in air. KB cells were seeded at a density of 5×10^4 cells/well in 96-well flat-bottomed plates. The cells were folate-starved using a folate-deficient special RPMI 1640 medium (modified RPMI 1640 without folic acid, vitamin B_{12} and phenol red; sigma) without FBS. Then, the cells were treated with 100 μg/ml of HL, FHL, or FHL plus 2 mM free folate. Following 1, 6, 12 and 24 h of incubation under 5% CO_2 at 37°C, the cells were washed with PBS and the cell viability was assessed by MTT colorimetric assay using automated microplate reader (570 nm; VERSAmax™, Molecular Devices Corp., Sunnyvale, CA).

Flow Cytometry Analysis

KB cells grown in a monolayer were incubated with indicated concentrations of UFH, HL or FHL. After 12 h, cells were collected, washed with 1 ml of PBS, and fixed by 1 ml of 70% ethanol with gentle vortexing. The cell pellet was resuspended in PI solution (50 μg/ml) at a concentration of 10^6 cells/ml, and maintained at room temperature for 30 min. DNA content was then analyzed by a flow cytometer (Beckton Dickinson, Franklin Lakes, NJ) and sub G1 period, called the apoptotic index, was observed. Results were calculated as means±s.d. from at least three individual experiments.

TUNEL Assay *In Vitro*

Apoptotic cells were evaluated by double staining for Annexin-V-Alexa Fluor 488 binding and propodium iodide incorporation using the Apoptosis Detection Kit (Invitrogen detection technologies, Carlsbad, CA). Single stain controls were performed before each analysis according to the standard protocol. Flow cytometry analysis was performed on 10,000 cells with a FACS Calibur (Becton Dickinson) and Cell Quest Pro software. For the terminal deoxynucleotidyl transferase-mediated dUTP nick end-labeling (TUNEL) assay, KB cells were plated on slide chamber and cultured in RPMI 1640 containing 10% FBS for 12 h. The culture medium was then replaced with folate-deficient special RPMI 1640 medium without FBS. Then, 100 μg/ml of UFH or HL were treated to the cells for 24 h. In addition, 50, 100 or 300 μg/ml of FHL without or with 2 mM free folate were also separately treated to the cells for 24 h. Apoptosis was assayed using the TMR Red *in situ* Apoptosis Detection Kit (Roche Diagnostic, Indianapolis, IN), and cells were counterstained with TOPRO-3 (Molecular Probes, Eugene, OR). Cells were then observed by fluorescence microscopy using an inverted microscope (LEICA TCS SP2 microscopy, Leica Microsystems GmbH, Wetzlar, Germany). Images were obtained with digital camera (model DM IRE2, Scientific. Inc., Germany) and Image-Pro Plus software. TUNEL positive cells were calculated as follows: (number of apoptotic nuclei/number of total nuclei) ×100. Three measurements were obtained from each border zone area by a single investigator blinded to the treatment group.

Experimental Tumor Graft Growth Models

Seven-week old female athymic BALB/C nude mice weighing 20–25 g were purchased from Charles River Laboratories (Wilmington, MA) and maintained on a folate-free rodent diet. Then, KB cells (1×10^7 cells/100 μl) were inoculated subcutaneously at the left flank of the animals. When the tumor size were reached to 70–100 mm^3, the mice were received following treatments: (a) 0.9% NaCl solution (normal saline) for control group, (b) HL (5 mg/kg) and (c) FHL (5 mg/kg), respectively. The drugs were given by intravenous injection on every third day for 2 weeks. Tumor sizes were daily monitored and tumor volumes were calculated as $a^2\times b\times0.52$, where a=width and b=tumor length.

Immunohistochemical Analysis

Tumor tissues of each group were isolated after 2 weeks and intratumoral microvessel density was then analyzed using a rat anti-mouse CD34 monoclonal antibody (Abcam, Cambrige, UK). Immunoperoxidase staining was done using the streptavidin-peroxidase method. As the final step, the nuclei of the sections were counterstained with hematoxylin solution. The image that contained the highest number of microvessels was chosen for each section from an initial scan at ×100 magnification. Then, the vessels were counted in the selected image at ×200 magnification. At least five fields were counted for each section. Two independent investigators evaluated the number of vessels. TUNEL assay was also performed with commercial kit (Roche Diagnostics) according to the manufacturer's instructions. The assay was performed in triplicate and repeated three times with five independent tumors from each treatment group. The percentage of apoptosis was calculated by dividing the number of TUNEL-positive cells with the total number of cells and multiplying the result by 100. The counting was performed in the ×100 magnification.

Statistics

Data are expressed as means ± standard deviation (s.d.). ANOVA test was used to compare groups and P values of <0.05 were considered significant.

RESULTS

Synthesis and Characterization of HL and FHL

We developed heparin amphiphiles by conjugating lithocholate as hydrophobic moieties to the hydrophilic heparin (Fig. 1). HL was initially prepared by covalent linkage of Lithocholate to heparin, and this resulted in lower anticoagulant activity (38%) than that produced by the unmodified heparin. The presence of lithocholate in HL was confirmed by ^{1}H NMR (400 MHz, CD_3OD/D_2O=2/1, v/v). The characteristic peaks of lithocholate appeared at 18-CH_3 (0.64 ppm), 19-CH_3 (0.91 ppm), 21-CH_3 (1.24 ppm), and the new amide linkage between heparin and lithocholic acid was observed at 8.04 ppm

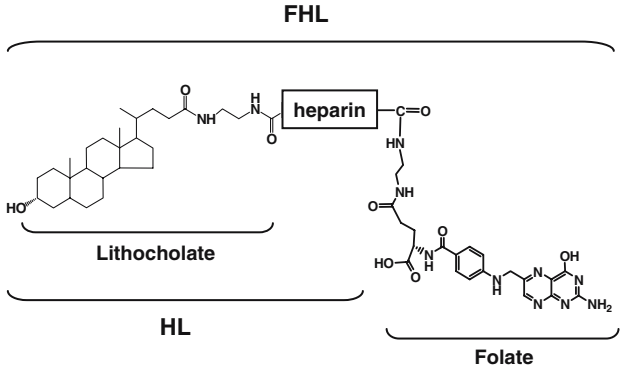

Fig. 1. Chemical structure of heparin-lithocholate (HL) and folate-heparin-lithocholate (FHL) conjugates.

(data not shown). This amide linkage was further confirmed at the wavelength of 1,665 cm^{-1} in the FT-IR spectra (data not shown). In addition, the peak that appeared near 2,360 cm^{-1} represented the stretching vibration of intrinsic sulfonamide ($-NHSO_3$) in heparin as previously reported (27). Folate conjugated HL (FHL) was then synthesized as shown in Fig. 1. This FHL also represented a low anticoagulant activity (28%). The average particle size of heparin amphiphiles in distilled water was about 170 nm (there was about 10 nm size change after the folate conjugation), and zeta potential values of HL and FHL were −50 and −25 mV, respectively.

In Vivo Matrigel Plugs Assay

In vivo antiangiogenic activities of HL and FHL were investigated by measuring the extent of blood vessel invasion into Matrigel plugs. As shown in Fig. 2, blood vessels were formed in the order of positive control (with bFGF only), UFH, FHL, HL and negative control (with PBS). Further estimation of hemoglobin content in the Matrigel plugs showed that HL or FHL significantly inhibited the vascularization inside the plugs with 29 and 43% of hemoglobin content, respectively, ($P<0.01$ vs. positive control). The inhibition effect of UFH was lower than that of HL or FHL although UFH significantly inhibited the vascularization induced by bFGF ($P<0.05$ vs. positive control).

Cytotoxicity of FHL Via Folate Receptor on KB Cells

In vivo cytotoxicity of FHL was evaluated in KB cells by MTT assay. After 24 h incubation with FHL (100 μg/ml), viable cells were only 25% ($P<0.001$), (Fig. 3A). However, the cytotoxicity of FHL in KB cells was not completely shown by treating free folate to block the binding of FHL to the FR. Furthermore, non-folate-conjugated HL did not affect cell viability. We examined the DNA content of cells to determine whether the cellular cytotoxicity of FHL is related with the induction of apoptosis. Cells populated at a sub-G1 phase, which is typically indicative of apoptosis (6), were evaluated by flow cytometry analysis (Fig. 3B and 3C). The treatment of 100 μg/ml of UFH or HL for 12 h did not induce the sub-G1 accumulation, whereas, cells in FHL revealed 3.2-fold higher sub-G1 population than in UFH. In addition, FHL treated cells in the sub-G1 period markedly were increased from 4.8 to 38.2% with increase in the culture time up to 24 h. In contrast, when we added 2 mM free folate to the medium, FHL did not significantly affect cell cycle as exhibited in cell viability.

We further evaluated the apoptotic effect of FHL to distinguish it from necrotic effect. It can be also used to quantify three populations of cells with drug treatment: normal viable cells, apoptotic cells, and populations of necrosis using Annexin V and PI staining. As shown in Fig. 3D, normal viable cells (AV−/PI−) are shown in the *bottom left window,* apoptotic cells (AV+/PI−) in the *bottom right window,* and the population of necrosis (AV+/PI+) in the *top right window*. Untreated cells yielded only 3% apoptotic cells; cells treated with UFH for 24 h showed 7% apoptotic cells; and cells treated with HL for 24 h showed 18% apoptotic cells. However, cells treated with FHL for 24 h showed 78% apoptotic cells. Cells in FHL also showed increased necrosis (11%) at 24 h, but it was not very high compared to the amount of increased apoptotic cells.

Cellular Internalization of FHL in KB Cells

We investigated that the intracellular delivery, which is the comparative cellular uptake, of FITC-labeled FHL occurred in a FR-mediated specific manner and that the apoptosis in cells have taken up FITC–FHL. Cells were incubated with FITC–FHL or FITC–HL (100 μg/ml) for 24 h to evaluate whether these molecules were taken up inside cells, and the TUNEL assay and nuclei staining using TOPRO-3 were carried out simultaneously to monitor apoptosis (Fig. 4). The cells incubated with FITC–FHL showed higher cellular uptake, especially in the nuclei, than those with HL, indicating that folate conjugation provide with the ability of cellular endocytosis. TUNEL-positive cells precisely matched those with FITC image and TOPRO-3 staining. These results imply that cells incubated with FHL were scored as apoptotic because they were affected by internalized heparin amphiphiles.

Inhibitory Effects of HL and FHL on Tumor Graft Growth

KB cells were subcutaneously implanted into the flanks of BALB/C nude mice, and subsequent tumor growth, neovascularization and apoptosis induction were monitored after intravenous injection of 5 mg/kg/3 day of HL or FHL for 14 days. As shown in Fig. 5, mice that received HL or FHL exhibited higher antitumor activity than control. Tumor growth suppression in FHL indicated improved therapeutic efficacy (69% of growth inhibition *versus* control) compared to the mice in non-folate HL (56% of growth inhibition *versus* control). However, there was not significant difference between FHL and HL in inhibiting tumor growth. To determine whether the reduced size of FHL- or HL-treated tumors coincides with reduction in neovascularization or apoptosis induction, we initially used five representative FHL-, HL-treated or saline-treated tumors to quantify the density of microvessels after immunostaining with anti-CD34 antibody. The reduced size of FHL- or HL-treated tumors was consistent with a decrease in CD34-positive microvessels, and the reduction ratio was 60 and 48% *versus* control, respectively, (Fig. 6A and B). Interestingly, FHL-treated tumors significantly showed 3.2-fold higher induction of apoptosis compare with HL-treated tumors ($P<0.001$) (Fig. 6C and D). However, this apoptotic level might not induce noticeably increased *in vivo* tumor regression as we confirmed in tumor volume result, demonstrating that the antiangiogenic effect of heparin amphiphiles might dominant *in vivo,* compared to the apoptotic effect.

DISCUSSION

We prepared the heparin-lithocholate conjugate (HL) comprised of covalently bound heparin, as a hydrophilic segment, and lithocholic acid as a hydrophobic segment. The amide formation between carboxyl groups of glucuronic acid and iduronic acid residues in heparin and amine groups of Litho-NH_2 was confirmed by ^1H NMR and IR.

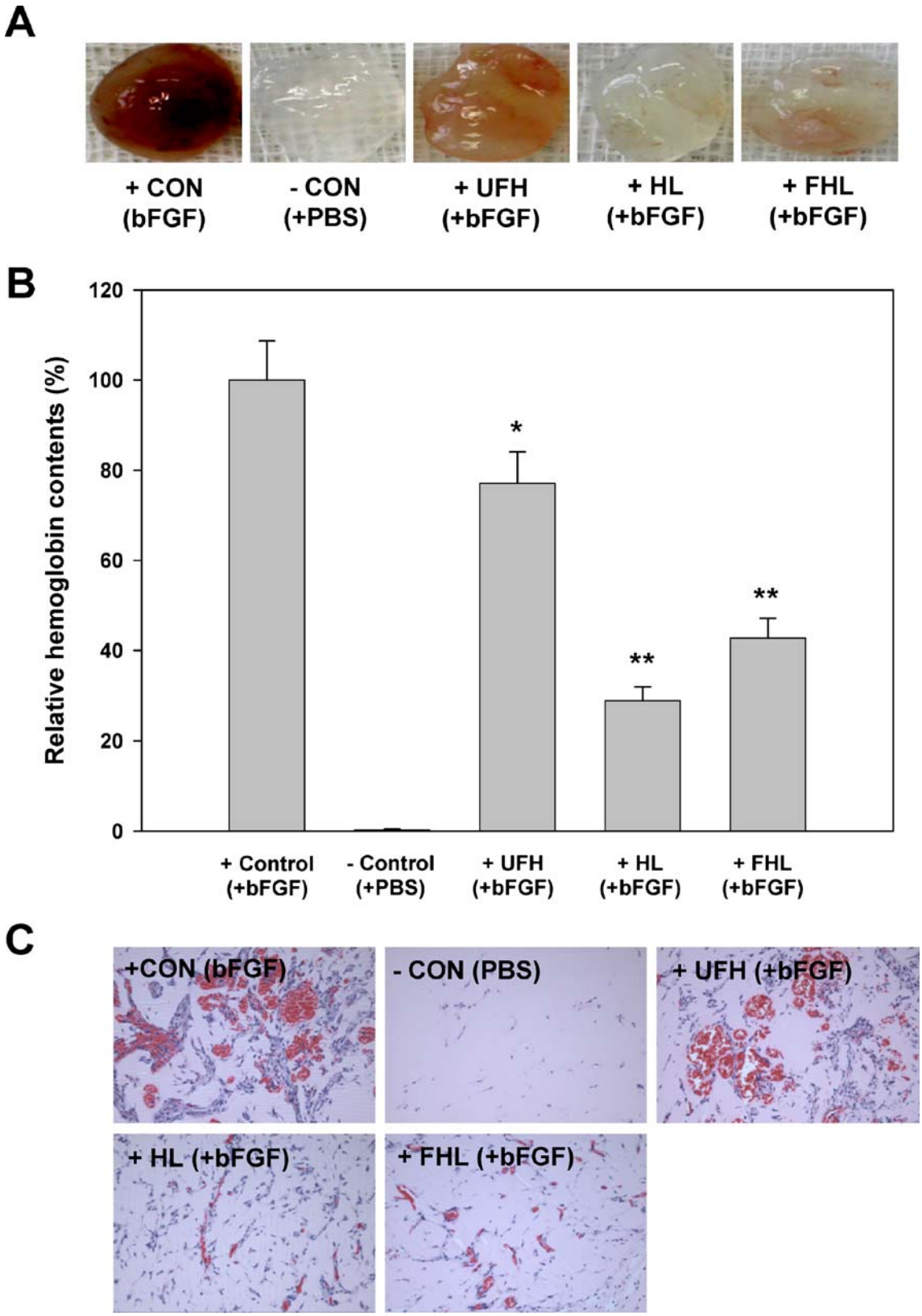

Fig. 2. *In vivo* antiangiogenic activities. **A** Matrigel plugs containing bFGF alone (+control), bFGF plus UFH, bFGF plus FHL, bFGF plus HL, or no bFGF (PBS,-control) were photographed. **B** Relative hemoglobin contents in Matrigel plugs determined by the Drabkin's method. Data were expressed as means±s.d. (N=5). (*P<0.05 *versus* + control, **P<0.001 *versus* + control). **C** Sections of each Matrigel plugs stained with H&E were examined by light microscopy (×200).

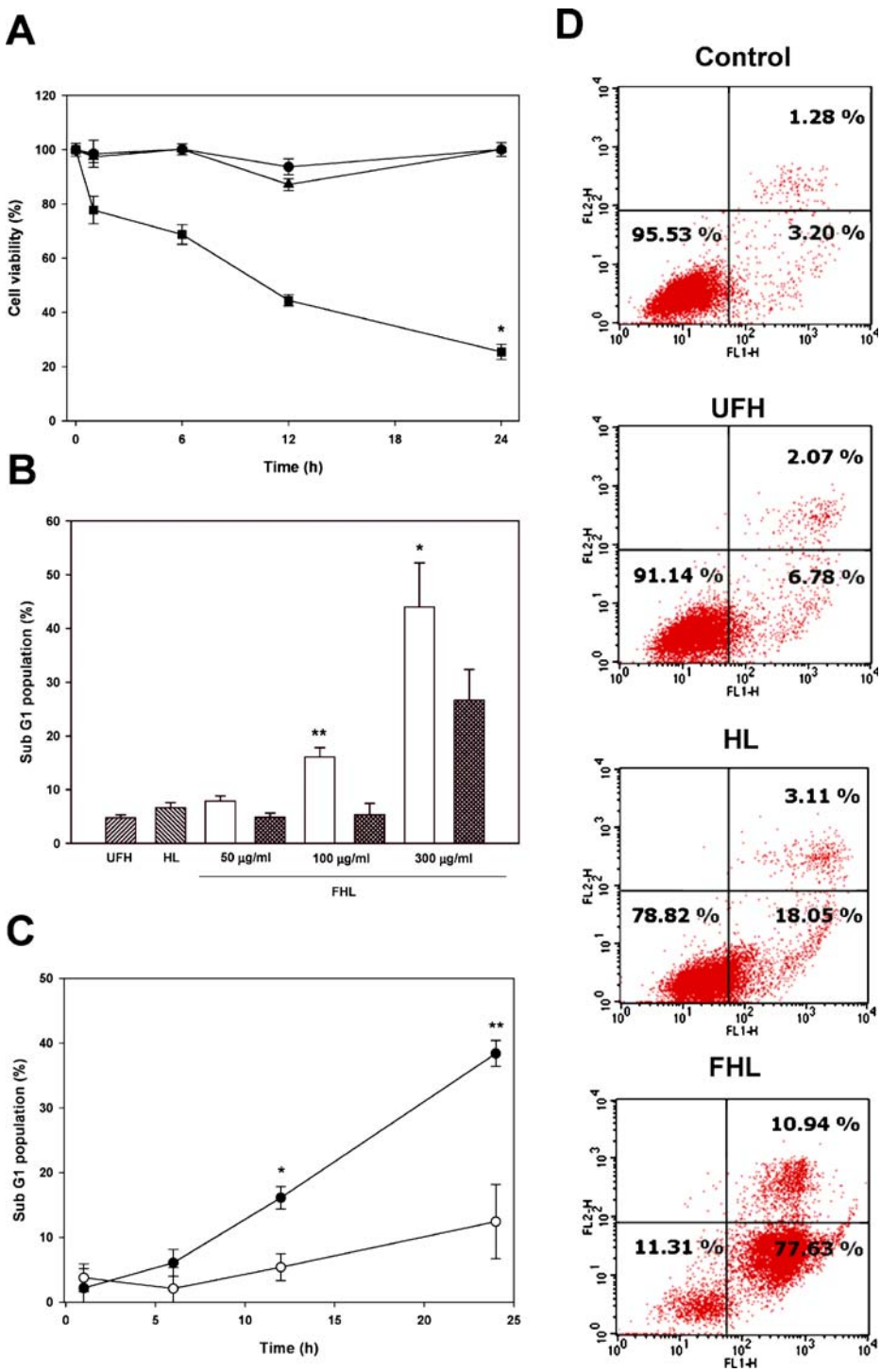

Fig. 3. Cellular cytotoxicity of HL and FHL in KB cells. **A** Cell viability of the KB cells treated with 100 μg/ml of HL (●), FHL (■) or FHL plus 2 mM free folate (▲) was measured by MTT assay. Data were expressed as means ± s.d. (N=5). (*P<0.001 *versus* FHL plus 2 mM free folate). **B** The sub-G1 population in KB cells treated with UFH (▨, 100 μg/ml), HL (▩, 100 μg/ml) or different doses of FHL(□) alone or plus 2 mM free folate (■) for 12 h. Data were expressed as means ± s.d. (N=3). (*P<0.05, **P<0.001 *versus* UFH). **C** The sub-G1 population in KB cells treated with 100 μg/ml of FHL (●) or FHL plus 2 mM free folate (○) at different treating times. Data were expressed as means ± s.d. (N=4). (*P<0.005, **P<0.002). **D** Flow cytometry analysis for apoptotic and necrotic KB cells stained with Annexin V (AV) and propidium iodide (PI) after treatment with 100 μg/ml of UFH, HL or FHL for 24 h. Viable cells (AV−/PI−) are in the *lower left-hand* quadrant. Early apoptotic cells (AV+/PI−) are in the *lower right-hand* quadrant. Terminal apoptotic/necrotic cells (AV+/PI+) are in the *upper right-hand* quadrant. Sizes of cell sub-populations are given as percentage of total populations.

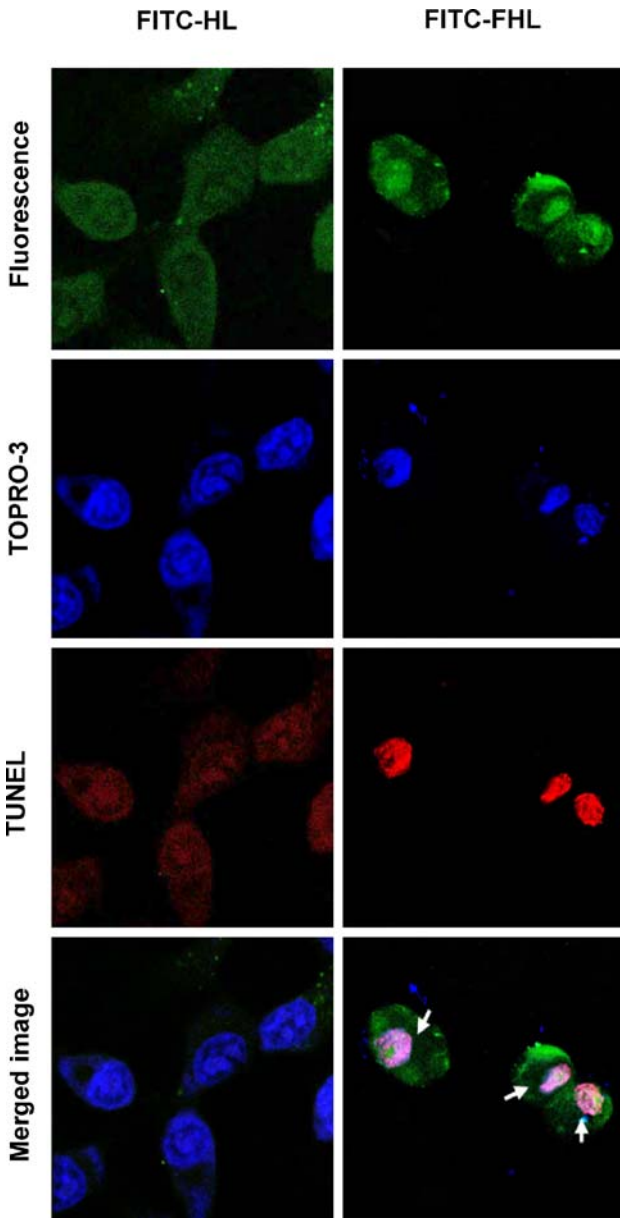

Fig. 4. Cellular internalization of FHL in KB cells microscope after treatment with 100 μg/ml of FITC-HL or FITC-FHL for 24 h. KB cells co-stained with TUNEL and TOPRO-3 stain were visualized by using confocal laser scanning. *Arrows*: FITC/TUNEL double positive cells.

In the aqueous condition, heparin amphiphiles were self-aggregated to make nanoparticles. Since negatively charged heparin might cover the core hydrophobic lithocholic acids as previously discussed (22), the ξ potential of self-aggregates were still negative (−50 mV). Folate conjugated HL (FHL) was synthesized by coupling folate to HL in order to bind to folate receptors in the tumor cell membrane. Both HL and FHL with a low anticoagulant characteristic are useful in long term delivery or at high dose because they can overcome several limitations noted in the administration of heparin; hemorrhage, thrombocytopenia, or osteoporosis etc. had been cited as problems of heparin treatment. It is important, however, that HL and FHL should retain their antiangiogenic ability and antitumoral efficacy since the sulfate groups, which play an important role in the binding with endothelial cells (28) or in blocking of FGF-heparan sulfate binding (11), were not modified.

In vivo Matrigel plugs assay showed that both HL and FHL had the lower hemoglobin content in the Matrigel than unmodified heparin in the bFGF induced vessel formation, implies that Both HL and FHL is more closely associated with bFGF than unmodified heparin, and decrease the activity of bFGF. Some literatures reported that suramin, the efficient angiosuppressive agent, blocked the receptor binding loop of the bFGFs through the hydrophobic interaction between the naphtyl or phenyl rings of the bound suramin and Pro, Cys, Gly, Arg, Gln, or Lys residues of bFGF (29), in addition to ion-pair, hydrogen bonding interactions, and van der Waals' contacts (30). These interactions provided the aggregates of suramin-bound bFGF, and made them to lose the activity of the bFGF for receptors, since hydrophobic residues of bFGF in receptor binding site have a crucial role for high affinity receptor binding (31). We speculate that the pronounced vessel formation inhibition of HL and FHL observed *in vivo* results from an additional coordinated mechanism, which efficiently inhibit the activity of growth factors, in particular basic fibroblast growth factor, through the hydrophobic interaction as well as ionic interaction.

In addition to mediating angiogenesis, FHL internalized into the cancer cells can be cytotoxic, and cause cancer cell death. We have shown that FHL treatment causes apoptosis in KB cells. FR-mediated delivery offers the physiological uptake of folate conjugated molecules by endocytosis, and provides them the chance to affect inside the cancer cells. Interestingly, FHL showed high cytotoxicity against KB cells, but neither HL nor FHL did so in the presence of excess free folate. Furthermore, high concentrations of HL (100 μg/ml) did not affect the viability of tumor cells up to 24 h. The cell cycle arrest within the sub-G1 phase was observed only in the FHL treated cells. UFH or HL, however, did not induce apoptotic cell population. Correspondingly, AV+ and PI-cells, one of the earliest markers of apoptotic death, were the most abundant in the exposure of cells to FHL. HL also represented early stages of apoptosis only by 18%, implying that the slight

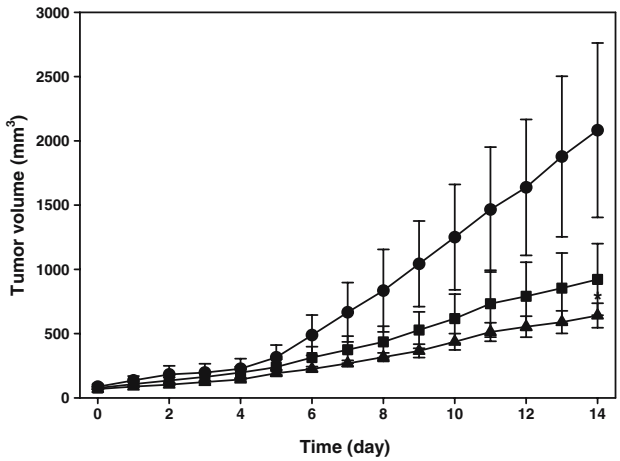

Fig. 5. Tumor graft growth curve during treating saline (●), HL (■; 5 mg/kg) or FHL (▲; 5 mg/kg) by intravenous injection Balb/c mice bearing KB cells via the lateral tail vein on every 3rd day for 2 weeks. Data were expressed as means ± s.d. (N=5). (*P<0.05 *versus* control).

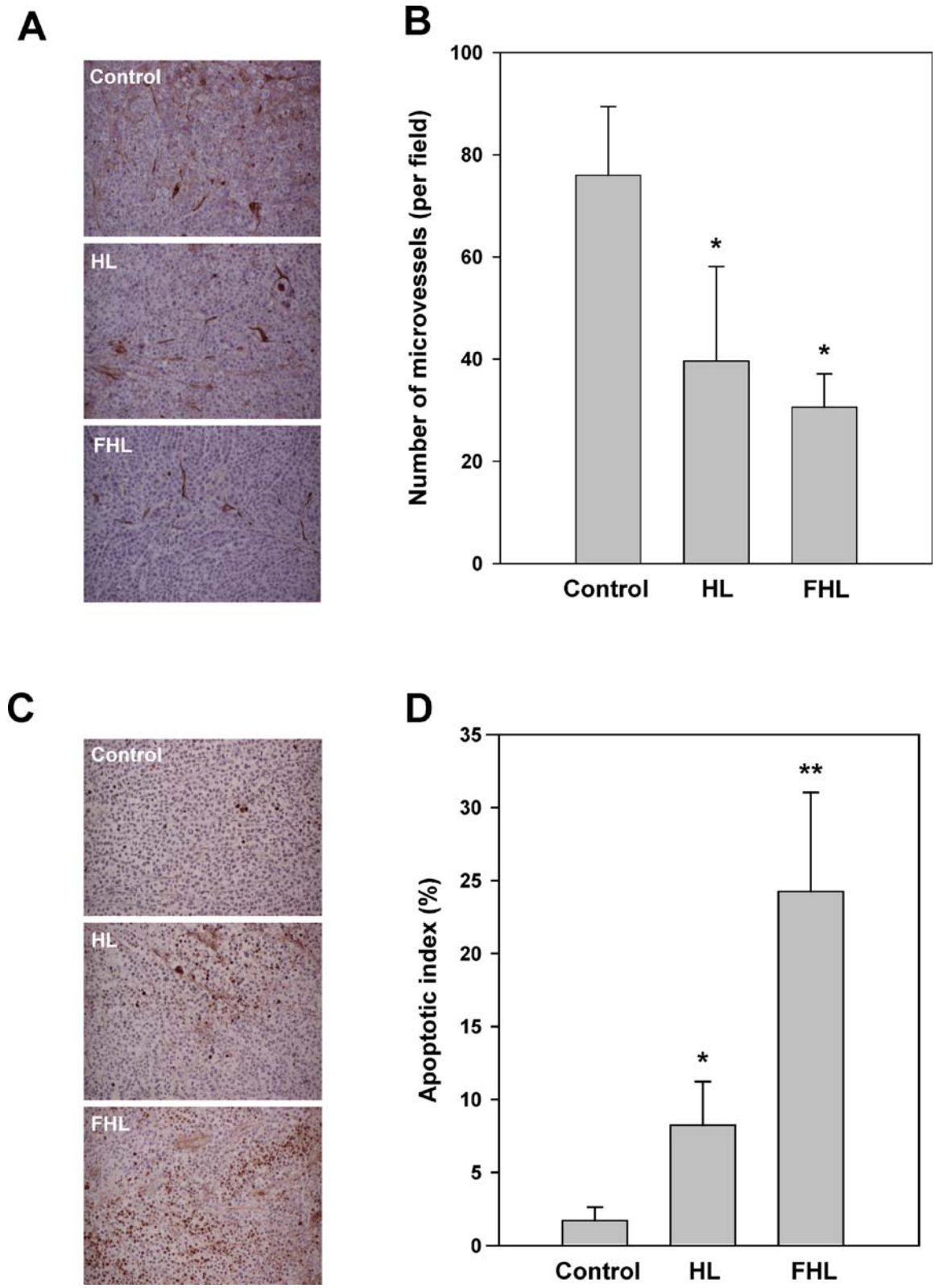

Fig. 6. Immunohistochemical analysis of tumor grafts. **A** Anti-CD34 immunostaining for microvessels in the tumor tissue after treatment of HL or FHL for 14 days. *Brown color*: Anti-CD34 positive microvessels. **B** The number of CD34 positive microvessels counted from the randomly selected fields of each tumor section in the ×100 magnification. Data were expressed as means ± s.d. (N=5) (*P<0.001 *versus* control). **C** TUNEL staining for apoptotic KB cells in the tumor tissue after treatment of HL or FHL for 14 days. *Brown color*: apoptotic cells. **D** The number of TUNEL positive cells counted from the randomly selected fields of each tumor section in the ×100 magnification. Percent apoptosis was calculated by dividing the total number of TUNEL-positive cells in each field (×100) by the total number of cells and multiplying by 100. Data were expressed as means ± s.d. (n=5). (*P<0.05 *versus* control, **P<0.001 *versus* control).

uptake might be possible due to its amphiphilic structure. In contrast, most of KB cells were not affected by UFH, because heparin internalization without any helper was unlikely; only 20 pg of internalized heparin was observed out of 1 μg/ml of heparin in 5×10^4 cells (8). Thus, the internalization of heparin amphiphiles into the cell seems to be an important factor for cellular apoptosis. TUNEL-FITC double staining clearly verified this mechanism. Notably, the uptake was concentrated on the nucleus, and this suggests that FHL escaped from endosome and might enter the nucleus. Several possible pathways involved in apoptosis of internalized heparin are rarely reported, such as interfering with transcription factor activity or activating the caspase−3/−7 (8), the inhibition of DNA binding by casein kinase II (32), and interfering with the polymerase chain reaction, which may involve DNA polymerase.

HL resulted in superior suppression of tumor growth as well as tumor angiogenesis compared with UFH in a mouse KB tumor model. The results of significantly diminished vessels in HL treated tumor were consistent with the result of Matrigel plugs assay, and HL leads to the tumor growth inhibition. In our previous study, we speculated that the pronounced tumor growth inhibition of heparin-bile acid conjugates observed from efficient inhibition of the activity of growth factors, in particular basic fibroblast growth factor, through the hydrophobic interaction as well as ionic interaction (33,34). Also, the antitumoral effect of FHL was similar to that of HL, even though it retains antiangiogenic properties and has additional apoptotic characteristics for the KB cells. Indeed, it is possible that the antitumorigenic effect of FHL is possibly due to both the inhibition of angiogenesis and the induction of apoptotic tumor cell death, however, the vascularization modulation may predominantly affect on *in vivo* system than the induction cancer cell death.

In this study, we firstly demonstrated that the internalization of heparin could induce apoptosis of cancer cells and report a novel anticancer therapeutic agent called FHL, which is an angiogenesis inhibitor combined with the apoptosis of tumor cell. Therefore, we expect that the exploitation of the effective internalization method of heparin like the folate conjugated heparin amphiphiles would provide a good opportunity for the development of a new class of anticancer agents.

ACKNOWLEDGEMENTS

This study was supported by the grant from Next Generation New Technology Development Program of the Korean Ministry of Commerce, Industry, and Energy (Grant no. 10011353).

REFERENCES

1. R. Sasisekharan, Z. Shriver, G. Venkataraman, and U. Narayanasami. Roles of heparan-sulphate glycosaminoglycans in cancer. *Nat. Rev., Cancer* **2**:521–528 (2002).
2. S. M. Smorenburg and C. J. NoordenVan. The complex effects of heparins on cancer progression and metastasis in experimental studies. *Pharmacol. Rev.* **53**:93–105 (2001).
3. M. Hejna, M. Raderer, and C. C. Zielinski. Inhibition of metastases by anticoagulants. *J. Natl. Cancer Inst.* **91**:22–36 (1999).
4. L. R. Zacharski and D. L. Ornstein. Heparin and cancer. *Thromb. Haemost.* **80**:10–23 (1998).
5. E. Erduran, Y. Tekelioglu, Y. Gedik, and A. Yildiran. Apoptotic effects of heparin on lymphoblasts, neutrophils, and mononuclear cells: results of a preliminary *in vitro* study. *Am. J. Hematol.* **61**:90–93 (1999).
6. H. L. Li, K. H. Ye, H. W. Zhang, Y. R. Luo, X. D. Ren, A. H. Xiong, and R. Situ. Effect of heparin on apoptosis in human nasopharyngeal carcinoma CNE2 cells. *Cell Res.* **11**:311–315 (2001).
7. S. J. Busch, G. A. Martin, R. L. Barnhart, and R. L. Jackson. Trans-repressor activity of nuclear glycosaminoglycans on Fos and Jun/AP-1 oncoprotein-mediated transcription. *J. Cell Biol.* **116**:31–42 (1992).
8. D. Berry, D. M. Lynn, R. Sasisekharan, and R. Langer. Poly(beta-amino ester)s promote cellular uptake of heparin and cancer cell death. *Chem. Biol.* **11**:487–498 (2004).
9. J. Hasan, S. D. Shnyder, A. R. Clamp, A. T. McGown, R. Bicknell, M. Presta, M. Bibby, J. Double, S. Craig, D. Leeming, K. Stevenson, J. T. Gallagher, and G. C. Jayson. Heparin octasaccharides inhibit angiogenesis *in vivo*. *Clin. Cancer Res.* **11**:8172–8179 (2005).
10. H. Engelberg. Actions of heparin that may affect the malignant process. *Cancer* **85**:257–272 (1999).
11. C. R. Parsish, C. Freeman, K. J. Brown, D. J. Francis, and W. B. Cowden. Identification of sulfated oligosaccharide-based inhibitors of tumor growth and metastasis using novel in vitro assays for angiogenesis and heparanase activity. *Cancer Res.* **59**:3433–3441 (1999).
12. K. Ono, M. Ishihara, K. Ishikawa, Y. Ozeki, H. Deguchi, M. Sato, H. Hashimoto, Y. Saito, H. Yura, A. Kurita, and T. Maehara. Periodate-treated, non-anticoagulant heparin-carrying polystyrene (NAC-HCPS) affects angiogenesis and inhibits subcutaneous induced tumour growth and metastasis to the lung. *Br. J. Cancer* **86**:1803–1812 (2002).
13. P. E. Thorpe, E. J. Derbyshire, S. P. Andrade, N. Press, P. P. Knowles, S. King, G. J. Watson, Y. C. Yang, and M. Rao-Bette. Heparin-steroid conjugates: new angiogenesis inhibitors with antitumor activity in mice. *Cancer Res.* **53**:3000–3007 (1993).
14. M. Gohda, T. Magoshi, S. Kato, T. Noguchi, S. Yasuda, H. Nonogi, and T. Matsuda. Terminally alkylated heparin. 2. Potent antiproliferative agent for vascular smooth muscle cells. *Biomacromolecules* **2**:1178–1183 (2001).
15. S. Miotti, S. Canevari, S. Menard, D. Mezzanzanica, G. Porro, S. M. Pupa, M. Regazzoni, E. Tagliabue, and M. I. Colnaghi. Characterization of human ovarian carcinoma-associated antigens defined by novel monoclonal antibodies with tumor-restricted specificity. *Int. J. Cancer* **39**:297–303 (1987).
16. L. R. Coney, A. Tomassetti, L. Carayannopoulos, V. Frasca, B. A. Kamen, M. I. Colnaghi, and V. R. Zurawski Jr.. Cloning of a tumor-associated antigen: MOv18 and MOv19 antibodies recognize a folate-binding protein. *Cancer Res.* **51**:6125–6132 (1991).
17. S. D. Weitman, R. H. Lark, L. R. Coney, D. W. Fort, V. Frasca, V. R. Zurawski Jr, and B. A. Kamen. Distribution of the folate receptor GP38 in normal and malignant cell lines and tissues. *Cancer Res.* **52**:3396–3401 (1992).
18. G. Toffoli, C. Cernigoi, A. Russo, A. Gallo, M. Bagnoli, and M. Boiocchi. Overexpression of folate binding protein in ovarian cancers. *Int. J. Cancer* **74**:193–198 (1997).
19. N. Parker, M. J. Turk, E. Westrick, J. D. Lewis, P. S. Low, and C. P. Leamon. Folate receptor expression in carcinomas and normal tissues determined by a quantitative radioligand binding assay. *Anal. Biochem.* **338**:284–293 (2005).
20. C. P. Leamon and P. S. Low. Folate-mediated targeting: from diagnostics to drug and gene delivery. *Drug Discov. Today* **6**:44–51 (2001).
21. J. Sudimack and R. J. Lee. Targeted drug delivery via the folate receptor. *Adv. Drug Deliv. Rev.* **41**:147–162 (2000).
22. K. Park, K. Kim, I. C. Kwon, S. K. Kim, S. Lee, D. Y. Lee, and Y. Byun. Preparation and characterization of self-assembled nanoparticles of heparin-deoxycholic acid conjugates. *Langmuir* **20**:11726–11731 (2004).

23. S. Wang, R. J. Lee, C. J. Mathias, M. A. Green, and P. S. Low. Synthesis, purification, and tumor cell uptake of ^{67}Ga-deferoxamine-folate, a potential radiopharmaceutical for tumor imaging. *Bioconjug. Chem.* **7**:56–62 (1996).
24. C. J. Mathias, S. Wang, P. S. Low, D. J. Waters, and M. A. Green. Receptor-mediated targeting of ^{67}Ga-deferoxamine-folate to folate-receptor-positive human KB tumor xenografts. *Nucl. Med. Biol.* **26**:23–25 (1999).
25. T. Chandy, G. S. Das, R. F. Wilson, and G. H. Rao. Use of plasma glow for surface-engineering biomolecules to enhance blood compatibility of Dacron and PTFE vascular prosthesis. *Biomaterials* **21**:699–712 (2000).
26. Y. Lee, H. T. Moon, and Y. Byun. Preparation of slightly hydrophobic heparin derivatives which can be used for solvent casting in polymeric formulation. *Thromb. Res.* **92**:149–156 (1998).
27. J. O. Nam, J. E. Kim, H. W. Jeong, S. J. Lee, B. H. Lee, J. Y. Choi, R. W. Park, J. Y. Park, and I. S. Kim. Identification of the αvβ3 integrin-interacting motif of βig-h3 and its anti-angiogenic effect. *J. Biol. Chem.* **278**:25902–25909 (2003).
28. T. Barzu, J. L. RijnVan, M. Petitou, P. Molho, G. Tobelem, and J. P. Caen. Endothelial binding sites for heparin. Specificity and role in heparin neutralization. *Biochem. J.* **238**:847–854 (1986).
29. P. A. Raj, E. Marcus, and R. Rein. Conformational requirements of suramin to target angiogenic growth factors. *Angiogenesis* **2**:183–199 (1998).
30. R. J. Linhardt. Heparin-induced cancer cell death. *Chem. Biol.* **11**:420–422 (2004).
31. O. Filhol, C. Cochet, and E. M. Chambaz. DNA binding activity of casein kinase II. *Biochem. Biophys. Res. Commun.* **173**:862–871 (1990).
32. E. Beutler, T. Gelbart, and W. Kuhl. Interference of heparin with the polymerase chain reaction. *Biotechniques* **9**:166–170 (1990).
33. K. Park, G. Y. Lee, Y. S. Kim, M. Yu, R. W. Park, I. S. Kim, S. Y. Kim, and Y. Byun. Heparin-deoxycholic acid chemical conjugate as an anticancer drug carrier and its antitumor activity. *J. Control. Release* **114**:300–306 (2006).
34. K. Park, Y. S. Kim, G. Y. Lee, J. O. Nam, S. K. Lee, R. W. Park, S. Y. Kim, I. S. Kim, and Y. Byun. Antiangiogenic effect of bile acid acylatedfs heparin derivative. *Pharm. Res.* **24**:176–185 (2007).